Development of High-Specificity Fluorescent Probes to Enable Cannabinoid Type 2 Receptor Studies in Living Cells

Roman C. Sarott,[a] Matthias V. Westphal,[a] Patrick Pfaff,[a] Claudia Korn,[b] David A. Sykes,[c] Thais Gazzi,[d] Benjamin Brennecke,[d] Kenneth Atz,[b] Marie Weise,[d] Yelena Mostinski,[d] Pattarin Hompluem,[c] Eline Koers,[c] Tamara Miljuš,[c] Nicolas J. Roth,[e] Hermon Asmelash,[e] Man C. Vong,[c] Jacopo Piovesan,[c] Wolfgang Guba,[b] Arne C. Rufer,[b] Eric A. Kusznir,[b] Sylwia Huber,[b] Catarina Raposo,[b] Elisabeth A. Zirwes,[b] Anja Osterwald,[b] Anto Pavlovic,[b] Svenja Moes,[b] Jennifer Beck,[b] Irene Benito-Cuesta,[f] Teresa Grande,[f] Samuel Ruiz de Martín Esteban,[f] Alexei Yeliseev,[g] Faye Drawnel,[b] Gabriella Widmer,[b] Daniela Holzer,[b] Tom van der Wel,[h] Harpreet Mandhair,[i] Cheng-Yin Yuan,[j] William R. Drobyski,[k] Yurii Saroz,[l] Natasha Grimsey,[l] Michael Honer,[b] Jürgen Fingerle,[b] Klaus Gawrisch,[g] Julian Romero,[f] Cecilia J. Hillard,[m] Zoltan V. Varga,[g,n] Mario van der Stelt,[h] Pal Pacher,[g] Jürg Gertsch,[i] Peter J. McCormick,[e] Christoph Ullmer,[b] Sergio Oddi,[o,p] Mauro Maccarrone,[p,q] Dmitry B. Veprintsev,[c] Marc Nazaré,[d] Uwe Grether,*[b] and Erick M. Carreira*[a]

[a]Laboratorium für Organische Chemie, Eidgenössische Technische Hochschule Zürich, Vladimir-Prelog-Weg 3, 8093 Zürich, Switzerland

[b]Roche Pharma Research & Early Development, Roche Innovation Center Basel, F. Hoffmann-La Roche Ltd., 4070 Basel, Switzerland

[c]Faculty of Medicine & Health Sciences, University of Nottingham, Nottingham NG7 2UH, UK; Centre of Membrane Proteins and Receptors (COMPARE), University of Birmingham and University of Nottingham, Midlands, UK

[d]Leibniz-Institut für Molekulare Pharmakologie FMP, Campus Berlin-Buch, 13125 Berlin, Germany

[e]William Harvey Research Institute, Barts and the London School of Medicine, Queen Mary University of London, London EC1M 6BQ, England

[f]Faculty of Experimental Sciences, Universidad Francisco de Vitoria, Pozuelo de Alarcón, 28223, Madrid, Spain

[g]National Institute on Alcohol Abuse and Alcoholism, National Institutes of Health, Rockville, MD 20852, USA

[h]Department of Molecular Physiology, Leiden Institute of Chemistry, Leiden University, 2333 CC, Leiden, The Netherlands

[i]Institute of Biochemistry and Molecular Medicine, University of Bern, 3012 Bern, Switzerland

[j]Department of Microbiology and Immunology, Neuroscience Research Center, Medical College of Wisconsin, Milwaukee, WI 53226, USA

[k]Department of Medicine, Neuroscience Research Center, Medical College of Wisconsin, Milwaukee, WI 53226, USA

[l]Department of Pharmacology and Clinical Pharmacology, School of Medical Sciences, Faculty of Medical and Health Sciences, University of Auckland, 1142 Auckland, New Zealand

[m]Department of Pharmacology and Clinical Pharmacology, Neuroscience Research Center, Medical College of Wisconsin, Milwaukee, WI 53226, USA

[n]HCEMM-SU Cardiometabolic Immunology Research Group, Department of Pharmacology and Pharmacotherapy, Semmelweis University, 1085 Budapest, Hungary

[o]Faculty of Veterinary Medicine, University of Teramo, 64100 Teramo, Italy

[p]European Center for Brain Research (CERC)/Santa Lucia Foundation, 00179 Rome, Italy

[q]Department of Medicine, Campus Bio-Medico University of Rome, 00128 Rome, Italy

Fluorescent Probe • G protein-coupled receptors • Cannabinoid Type 2 Receptor (CB$_2$R) • CNR2 • TR-FRET• FACS • confocal microscopy • binding kinetics

ABSTRACT: Pharmacological modulation of cannabinoid type 2 receptor (CB$_2$R) holds promise for the treatment of numerous conditions, including inflammatory diseases, autoimmune disorders, pain, and cancer. Despite the significance of this receptor, researchers lack reliable tools to address questions concerning the expression and complex mechanism of CB$_2$R signaling, especially in cell-type and tissue-dependent context. Herein, we report for the first time a versatile ligand platform for the modular design of a collection of highly specific CB$_2$R fluorescent probes, used successfully across applications, species and cell types. These include flow cytometry of endogenously expressing cells, real-time confocal microscopy of mouse splenocytes and human macrophages, as well as FRET-based kinetic and equilibrium binding assays. High CB$_2$R specificity was demonstrated by competition experiments in living cells expressing CB$_2$R at native levels. The probes were effectively applied to FACS analysis of microglial cells derived from a mouse model relevant to Alzheimer's disease and to the detection of CB$_2$R in human breast cancer cells.

Introduction

There is currently great interest in the endocannabinoid system (eCB system) and associated signaling pathways in relation to the chemistry of life as well as in the context of developing new therapies. The eCB system is a complex lipid signaling network found in all vertebrates and consists of cannabinoid receptors (CBRs), their endogenous ligands (endocannabinoids), enzymes involved in ligand biosynthesis and degradation, as well as endocannabinoid transporters.[1] Cannabinoid type 1 and 2 receptors (CB$_1$R and CB$_2$R) are class A G protein-coupled receptors (GPCRs) and have been shown to be involved in numerous physiological processes and disease states.[2–4] They share 44% overall and 68% homology in the ligand-binding domain.[3] Notably, CB$_1$R is the most abundant GPCR in the central nervous system and mediates the psychotropic effects associated with *Cannabis* consumption mainly through the action of (–)-Δ^9-*trans*-tetrahydrocannabinol ((–)-Δ^9-THC).[5] CB$_2$R is predominantly expressed in the periphery, largely by cells of the immune system,[6,7] and is considered a highly promising target for the treatment of tissue injury and inflammation,[8,9] as well as neurodegenerative diseases such as Alzheimer's disease (AD) and multiple sclerosis.[10,11] Although several structurally distinct CB$_2$R agonists have shown promising effects in animal disease models, none has so far succeeded in the clinic,[12] stressing the need for better fundamental understanding of CB$_2$R chemistry, biology, and medicine.[10] The ability to address important questions is hampered by the lack of reliable biological tools such as receptor specific antibodies,[13–15] and the highly inducible nature of CB$_2$R expression as a function of disease state[16–18] further complicates its biochemical and biophysical analysis.

Small molecule-based probes will help to interrogate CB$_2$R function, mechanism of action, biased signaling, expression levels and protein distribution in health and disease.[19] Of particular interest are fluorescent probes, which allow for real-time monitoring of ligand-receptor interactions and protein visualization with high spatiotemporal precision.[20–22] Several fluorescent ligands targeting CB$_2$R have been reported.[23–35] However, in our collective experience the published probes perform less than optimally as judged by at least one of the following criteria: modularity of design for multiple applications, selectivity over CB$_1$R, affinity and specificity for CB$_2$R, photophysical properties, and applicability across species, techniques, and cell types. Furthermore, bifunctional probes that require additional manipulations prior to imaging are often incompatible with live cells.[36,37]
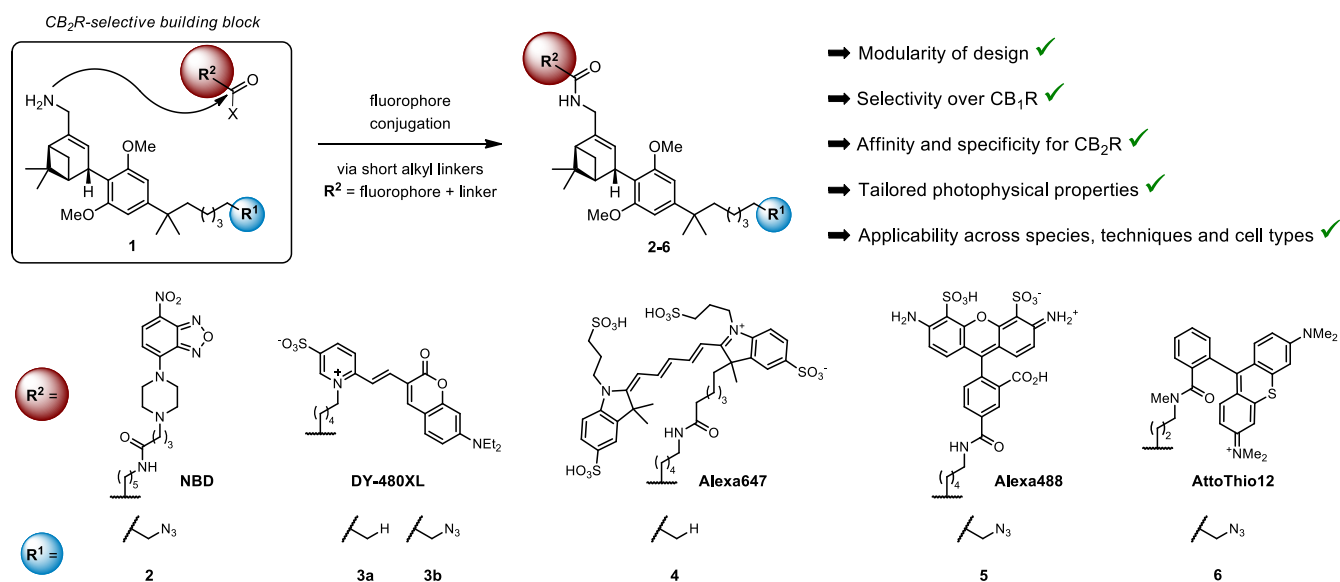

Figure 1. Modular design of CB$_2$R fluorescent probes. Attachment of fluorescent dyes to amine building block **1** via short linkers gives rise to CB$_2$R selective fluorescent probes with bespoke photophysical properties.

Recently, we reported the synthesis of HU-308-derived[38] primary amine **1** (Fig. 1), which was linked via R^2 to residues such as alkynes, diazirines, azobenzene photoswitches, and 7-nitrobenzofurazan (NBD) dye (**2**). These were evaluated in limited *in vitro* pharmacology (CB$_2$R and CB1R K$_i$, cAMP). However, the preliminary studies were largely synthetic in nature and did not assess **2** as a fluorescent probe. Herein, we report the modular synthesis and in-depth pharmacological evaluation of a series of CB$_2$R specific, high-affinity fluorescent probes. We also document their *in situ* application and validation in flow cytometry and real-time confocal microscopy of both living human and murine cells. Additionally, these probes proved effective in TR-FRET (Time Resolved Fluorescence Resonance Energy Transfer)-based assays allowing for determination of both binding affinities and kinetic parameters of CB$_2$R ligands without radiolabeled material. Finally, the probes are successfully applied to FACS analysis of cells from a mouse model of Alzheimer's disease, as well as to human breast cancer cells.

Results and Discussion

Modular Probe Design and *in vitro* Pharmacology.

With a high-affinity recognition element, such as **1**,[39] as a starting point, choice of the exit vector and linker-type for fluorophore attachment are the main challenges to ensure high probe affinity and selectivity.[40,41] Our preliminary synthetic studies with **2** suggested a strategy for a family of fluorescent probes.[42] Consequently, herein we report a series of probes **3a**–**6** in which the fluorescent dye was varied (Fig. 1, for synthetic details see SI). Fluorophores DY-480XL,[43] Alexa647,[44] Alexa488[45] and AttoThio12[46] were chosen for their large Stokes shift, red shifted absorption and emission maxima with high extinction coefficient, suitability for FRET, and potential for ultra-high resolution microscopy, respectively (for fluorescence spectra see SI Fig. S1 and Table S1). We focused on high-affinity azides **3b**, **5**, and **6**, as well as, for comparison, hydrocarbon analogs **3a** and **4**.

All fluorescent probes were subjected to *in vitro* pharmacological profiling in order to evaluate their affinity for CB_2R and selectivity over CB_1R (Table 1). Radioligand competition binding studies were performed with tritiated CP55,940 and membrane preparations of Chinese hamster ovary (CHO) cells overexpressing human (hCB_2R) or mouse CB_2R (mCB_2R), or human CB_1R (hCB_1R). Compounds **3a**, **3b**, **5** and **6** showed high to excellent affinity to hCB_2R, exhibiting K_i values of 99, 21, 268 and 4.7 nM, respectively, as well as good selectivity over hCB_1R, with hCB_1R/hCB_2R K_i ratios of 41, 113, >37 and 228, respectively. The presence of the terminal azide in **3b** led to a significantly higher binding affinity for hCB_2R as well as boosted selectivity over hCB_1R when compared to **3a**. To the best of our knowledge, the high selectivity of **3b** and **6** over hCB_1R is unprecedented for fluorescent CB_2R *agonists*, as discussed below.

In 2019, Liu and co-workers reported the X-ray crystal structure of CB_2R in its inactive state, determined in complex with antagonist AM10257.[47] We used this structure in docking studies of DY-480XL probe **3b**. The docking pose suggests that the fluorophore is positioned in the extracellular space (Fig. 2). In addition, the model predicts a hydrogen-bond between the amide-proton of **3b** and the carbonyl oxygen of
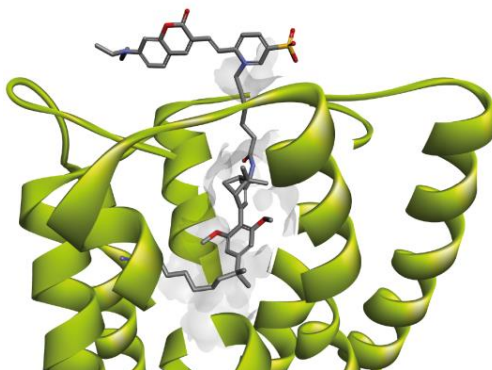

Figure 2. CB₂R Docking Studies. Probe **3b** was docked into inactive state CB_2R crystal structure (PDB: 5ZTY).

Ser90, which contributes to the high affinity of the probe.[39] When the docking pose of **3b** was compared with the recently published co-crystal structure of active state CB_2R in complex with agonist WIN55,212-2[48] the binding mode of the docked core motif was found to be identical, and the hydrogen bond with Ser90 was maintained.

In functional studies, probe **3b** showed agonist activity with high efficacy (hCB_2R cAMP EC_{50} = 171 nM, %eff = 150). A comparable value for **3b**, EC_{50} = 133 nM, was obtained in a [^{35}S]GTP-γ-S G protein activation study using hCB_2R expressed in *E. coli* membranes (see SI Fig. S2). AttoThio12 probe **6** performed best in terms of affinity and selectivity, displaying single digit nanomolar hCB_2R K_i as well as 228-fold selectivity over hCB_1R. In a cAMP assay **6** displayed lower efficacy, showing a trend towards partial agonism, and high functional selectivity over hCB_1R: hCB_2R cAMP EC_{50} = 5.6 nM, hCB_1R/hCB_2R EC_{50} ratio >1,785. The weaker affinity of Alexa647 probe **4** to hCB_2R was unexpected as it showed excellent CB_2R specificity in live-cell flow cytometry at concentrations below its apparent K_i, as discussed below. In forskolin-stimulated cAMP assay, **4** exhibited potent agonism: hCB_2R cAMP EC_{50} = 25 nM and hCB_1R/hCB_2R EC_{50} ratio = 86.

To check for interspecies differences that could compromise transferability of preclinical data from animal models to humans, binding studies were also performed with mCB_2R.[49] Probes **3a**, **3b**, **4** and **5** showed reduced binding affinities to mCB_2R compared to hCB_2R, while **6** retained single digit nanomolar affinity to mCB_2R, K_i = 1.1 nM. To

identify potential off-targets, compound **3b** was screened against a customized panel of 50 representative proteins.[50] In this assay, **3b** exhibited a very clean profile showing only a weak interaction with prostaglandin F receptor, which was considered not relevant due to the high test concentration of 10 µM (see SI Table S2).

In summary, modular fluorophore attachment to linchpin **1** gave rise to a series of high-affinity CB₂R selective fluorescent probes with bespoke photophysical properties. With several high-affinity and selective CB₂R fluorescent probes in hand, we set out to interrogate their utility in biological applications with a strong focus on validation across various laboratories and cell lines.

Table 1. *In vitro* pharmacological assessment of CB₂R fluorescent probes.[a]

Cmpd.	dye	K_i [nM]				EC_{50} [nM]			
		hCB_2R	hCB_1R	mCB_2R	hK_i ratio (CB_1R/CB_2R)	hCB_2R	hCB_1R	mCB_2R	EC_{50} ratio (CB_1R/CB_2R)
2	NBD	4.2	>10,000	n.d.[b]	>2,381	n.d.	n.d.	n.d.	n.d.
3a	DY-480XL	99	4,031	1,986	41	>10,000	>10,000	>10,000	n.d.
3b	DY-480XL	21	2,378	1,459	113	171 (150)	>10,000	118 (115)	>58
4	Alexa647	2,565	>10,000	>10,000	>3.9	25 (109)	2,152 (138)	370 (123)	86
5	Alexa488	268	>10,000	1,204	>37	n.d.	n.d.	n.d.	n.d.
6	AttoThio12	4.7	1,075	1.1	228	5.6 (74)	>10,000	17 (73)	>1,785

[a] Binding affinity (K_i) values were determined by a radioligand binding assay utilizing radioligand [³H]-CP55,940 and membrane preparations from CHO cells overexpressing hCB_1R, hCB_2R, or mCB_2R. Forskolin-stimulated cAMP (EC_{50}) levels were measured using cells stably expressing hCB_2R, mCB_2R or hCB_1R. Figures in parentheses correspond to efficacy expressed in % relative to 1 µM CP55,940. [b] n.d. - not determined.

TR-FRET-Based Determination of Equilibrium and Kinetic Binding Parameters: Radioligand-free Assay

Radioligands are ubiquitously used to study GPCR expression as well as ligand binding affinities and kinetics.[51] Safety concerns, radioactive waste management, and, in the case of filtration assays, the need for iterative washing steps limit the applicability of radioligand-based assays for high throuput screening (HTS). Fluorescent probes are devoid of such drawbacks and thus, in conjunction with FRET-based assays, offer an attractive solution towards the development of high throughput equilibrium binding assays.[52–56] In addition, time-resolved methods (TR-FRET) enable studying ligand binding kinetics, one of the key determinants of drug efficacy and safety.[57–62]

Towards this end, Human Embryonic Kidney (HEK293T-Rex) cells overexpressing SNAP-tagged hCB_2R were labeled with a SNAP-Lumi4-Tb FRET-donor (see SI). Laser excitation (337 nm) of this donor initiates energy transfer (FRET) to a proximal fluorescent probe acceptor. Membrane preparations of the derived cells were used to determine the binding kinetics of the most promising fluoroprobes **3b** and **6** using TR-FRET technique by measuring the observed association rates k_{obs} at various ligand concentrations, as shown for **3b** in Fig. 3A (for analogous results with **6** see SI). The observed rate of association was found to be linearly correlated to fluorescent probe concentration, as shown in Fig. 3B for **3b**. The kinetic rate parameters k_{off} and k_{on} for the two probes were calculated by globally fitting the association time courses. The ratio of these parameters, k_{off}/k_{on}, is equivalent to the ligand dissociation constant K_d. Saturation binding analysis provided an additional means for determining binding constants as shown for **3b** in Fig. 3C. Reassuringly, the two sets of K_d values were in good agreement: 35 vs 36 nM for **3b**, 18 vs 13 nM for **6** as shown in Table 2.

Additionally, good correlation was found between K_i values for **3b**, **4**, and **6** determined independently by FRET and by radioligand studies. Together with microscopy data showing membrane localization of SNAP-hCB_2R, this correlation justified the use of SNAP-tagged hCB_2R for further studies (see SI Fig. S4 and S5).

We next set out to validate **3b** and **6** as fluorescent alternatives to radioligand tracers. Binding affinities for established CB₂R-selective agonist HU-308 and inverse agonist SR144528[63] were determined in competition experiments with fluorescent probes **3b** and **6**. The results are summarized in Table 3 with competition binding curves for HU-308 and SR144528 obtained with probe **3b** presented in Fig. 3D. Of note, K_i values obtained in this manner agree with previously published benchmark values based on radioligand binding assays.[19] Furthermore, the same

experimental set up also allowed for successful determination of kinetic binding parameters of HU-308 and SR144528. Data obtained with **3b** in competitive association experiments are presented in Fig. 3E and 3F, and the observed binding parameters are summarized in Table 3. The determined kinetic rate constants are in good agreement with literature data derived using a CB$_2$R selective radioligand.[51] As compared to HU-308, the higher affinity of SR144528 to hCB$_2$R is driven by a faster on-rate, with otherwise equivalent off-rates.

To the best of our knowledge, this work is the first study of ligand binding kinetics for CB$_2$R specific ligands determined by TR-FRET. Fluorescent probes **3b** and **6** are attractive alternatives to radioligands for the study of binding kinetics and affinities of unlabeled ligands to hCB$_2$R, and they are promising for HTS applications.
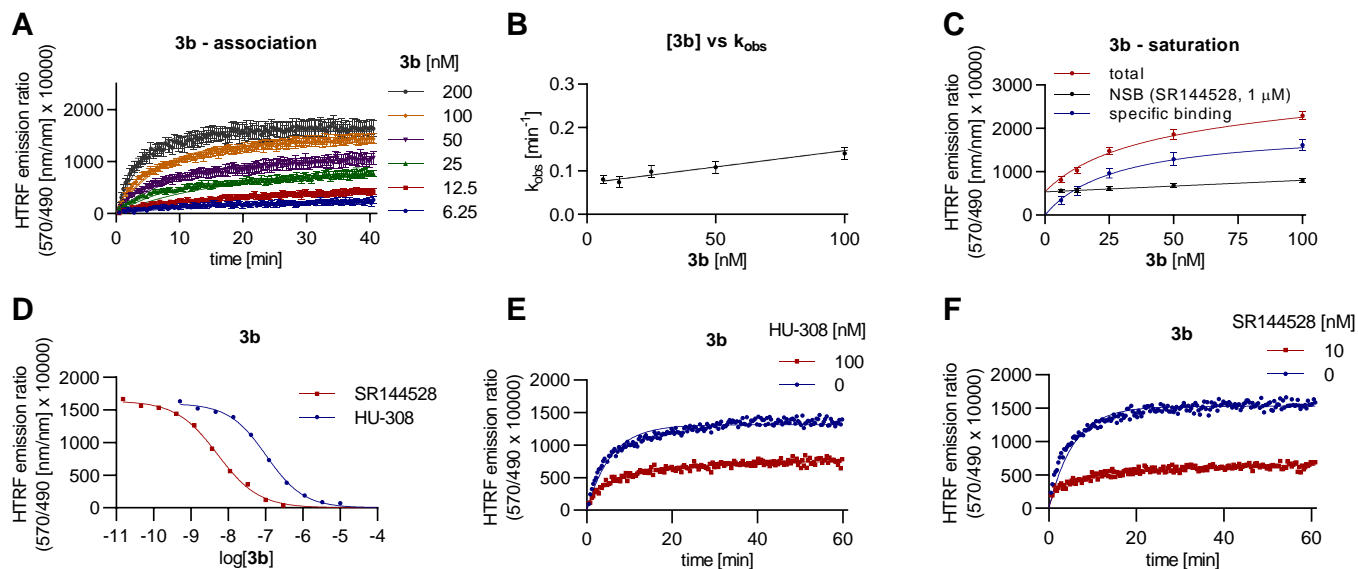

Figure 3. TR-FRET-based fluorescent probe characterization (A-C) and determination of affinities and binding kinetics of CB$_2$R ligands (D-F). A) Observed association of **3b** to hCB$_2$R. B) Observed association rate, k_{ob}, increases linearly with **3b** concentration C) Saturation analysis showing the binding of **3b** to hCB$_2$R. **D)** Competition between **3b** (100 nM) and increasing concentrations of CB$_2$R selective ligands HU-308 and SR144528 for hCB$_2$R. Probe **3b** competitive association curves in the presence of HU-308 E) and SR144528 F). Kinetic and equilibrium data were fitted to the equations described in the SI to calculate K_d, k_{on} and k_{off} values for fluorescent and for unlabeled ligands. Data are summarized in Tables 2 and 3, and are presented as mean ± SEM, N = 3-5.

Table 2. Binding Parameters of Fluorescent Probes to hCB$_2$R as determined by TR-FRET.[a]

Cmpd.	k_{on} [10^6 M^{-1} min^{-1}]	k_{off} [min^{-1}]	Kinetic K_d [nM]	Saturation K_d [nM]
3b	1.2 ± 0.1	0.04 ± 0.01	35 ± 7	36 ± 4
6	1.9 ± 0.5	0.03 ± 0.05	18 ± 3	13 ± 2

[a] Data are presented as mean ± SEM, N = 3-5.

Table 3. Kinetic and affinity binding parameters of ligands for hCB$_2$R as determined by TR-FRET.[a]

Probe	HU-308					SR144528				
	k_{on} [10^6 M^{-1} min^{-1}]	k_{off} [min^{-1}]	RT [min]	Kinetic K_d [nM]	K_i [nM]	k_{on} [10^7 M^{-1} min^{-1}]	k_{off} [min^{-1}]	RT [min]	Kinetic K_d [nM]	K_i [nM]
3b	3.43 ± 1.34	0.15 ± 0.02	6.7	55 ± 15	23 ± 5	5.17 ± 1.26	0.12 ± 0.03	8.3	2.3 ± 0.3	1.5 ± 0.4
6	2.22 ± 0.84	0.10 ± 0.02	10	53 ± 12	153 ± 24	4.11 ± 1.28	0.12 ± 0.04	8.3	3.1 ± 0.3	4.9 ± 1.2

[a] Data are presented as mean ± SEM, N = 3.

CB₂R-Specificity in Living CHO, Human and Murine Cells: FACS Studies.

We set out to investigate the specificity of the fluorescent probes by flow cytometry. This included CHO cells over-expressing hCB₂R, mCB₂R or hCB₁R along with wild-type CHO cells, which were incubated with fluorescent probes at varying concentrations. In subsequent FACS analyses, cells expressing hCB₂R or mCB₂R treated with **3b** showed increased mean fluorescence intensity compared to cells expressing hCB₁R, as well as wild-type cells. The increased fluorescence signal was statistically significant at **3b** concentrations >3.33 µM ($p < 0.005$, also see SI Fig. S6). Alexa488 probe **5** performed particularly well, and specifically labelled both CHO cells expressing mCB₂R and hCB₂R over a broad concentration range of 0.12 – 10 µM (Fig. 4A). Additionally, Alexa647 probe **4** showed a significant increase of fluorescence intensity for cells expressing hCB₂R over a concentration range of 0.37 µM – 10 µM (see SI Fig. S6). It is interesting to note that the performance of **4** in FACS is somewhat at odds with its K_i value of 2.57 µM. We speculate that two factors are responsible: (1) high fluorescence intensity of Alexa647 and (2) minimal nonspecific binding by the highly charged dye as noted previously.[64]
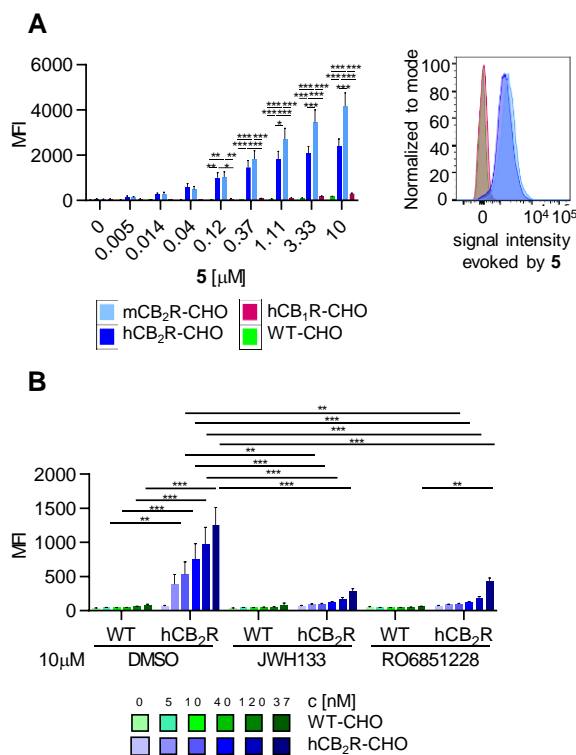

Figure 4. A) FACS analysis of cells incubated with **5** at varying concentrations. MFI = mean fluorescence intensity. Representative fluorescent intensity histograms of cells incubated with 0.37 µM **5**. Mean ± SEM, two-way ANOVA, * $p<0.05$; ** $p<0.01$; *** $p<0.005$, N = 4-5. B) FACS analysis of cells pre-treated with 10 µM of competitor ligands and subsequently stained with varying concentrations of **5**. Mean ± SEM, Two-way ANOVA, * $p<0.05$; ** $p<0.01$; *** $p<0.005$, N = 3-5.

Nonspecific membrane binding is a major concern of commonly employed CB₂R ligands, which most often are highly lipophilic in nature. Consequently, additional experiments were performed to investigate the specificity of our fluorescent probes. In particular we examined whether pre-incubation of cells with CB₂R agonist JWH133 and inverse agonist RO6851228[65] prior to FACS analysis interferes with fluoroprobe binding. Both CB₂R ligands competed with probe **3b** in a concentration-dependent fashion, supporting its high target specificity (see SI Fig. S6). Similarly, they efficiently displaced Alexa488 probe **5** (Fig. 4B) as well as Alexa647 probe **4** (see SI Fig. S6). To the best of our knowledge, these data in flow cytometry represent the first successful ligand displacement experiments of CB₂R fluorescent probes by validated CB₂R ligands.

We subsequently set out to investigate the specificity of the fluorescent probes in two living, clinically relevant, human and murine cell lines. Probe **3b** successfully labelled activated microglial cells from 5xFAD mice. These mice recapitulate phenotypes related to Alzheimer's disease (AD) such as amyloid plaques and increased expression of mCB₂R in the CNS.[66,67] The use of microglia derived from CB₂R knock-out (CB₂KO) mice led to significantly weaker labeling in flow cytometry, which corroborates the CB₂R specificity of **3b** in this murine AD model (Fig. 5). Compound **3b** also labeled human MDA-MB-231 breast cancer cells, expressing hCB₂R endogenously (see SI Fig. S7).
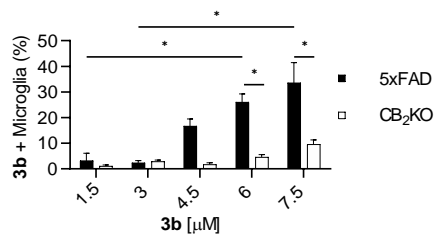
Figure 5. Fluoroprobe **3b** specifically labels mCB$_2$R on activated microglial cells from AD mice (5xFAD). Shown is the percentage of microglial cells positive for **3b**. *p<0.05 (two-way ANOVA followed by Tukey's post hoc analysis, N = 4–12).

Real-Time Receptor Visualization in Living Cells: Confocal Fluorescence Microscopy Studies

Based on the high CB$_2$R-specificity of the fluorescent probes in FACS, the suitability of **3b** to visualize cell-surface CB$_2$R was assessed by real-time confocal microscopy. Exposure of CHO cells overexpressing hCB$_2$R to **3b** resulted in distinct time- and concentration-dependent labeling of the cell membrane. Labeling with 0.2 µM **3b** was detectable within 5 min and increased progressively over time, reaching a steady-state plateau after 8 min and then remained unchanged, without evidence of internalization, for up to 10 min (Fig. 6A, also see Supplementary Video
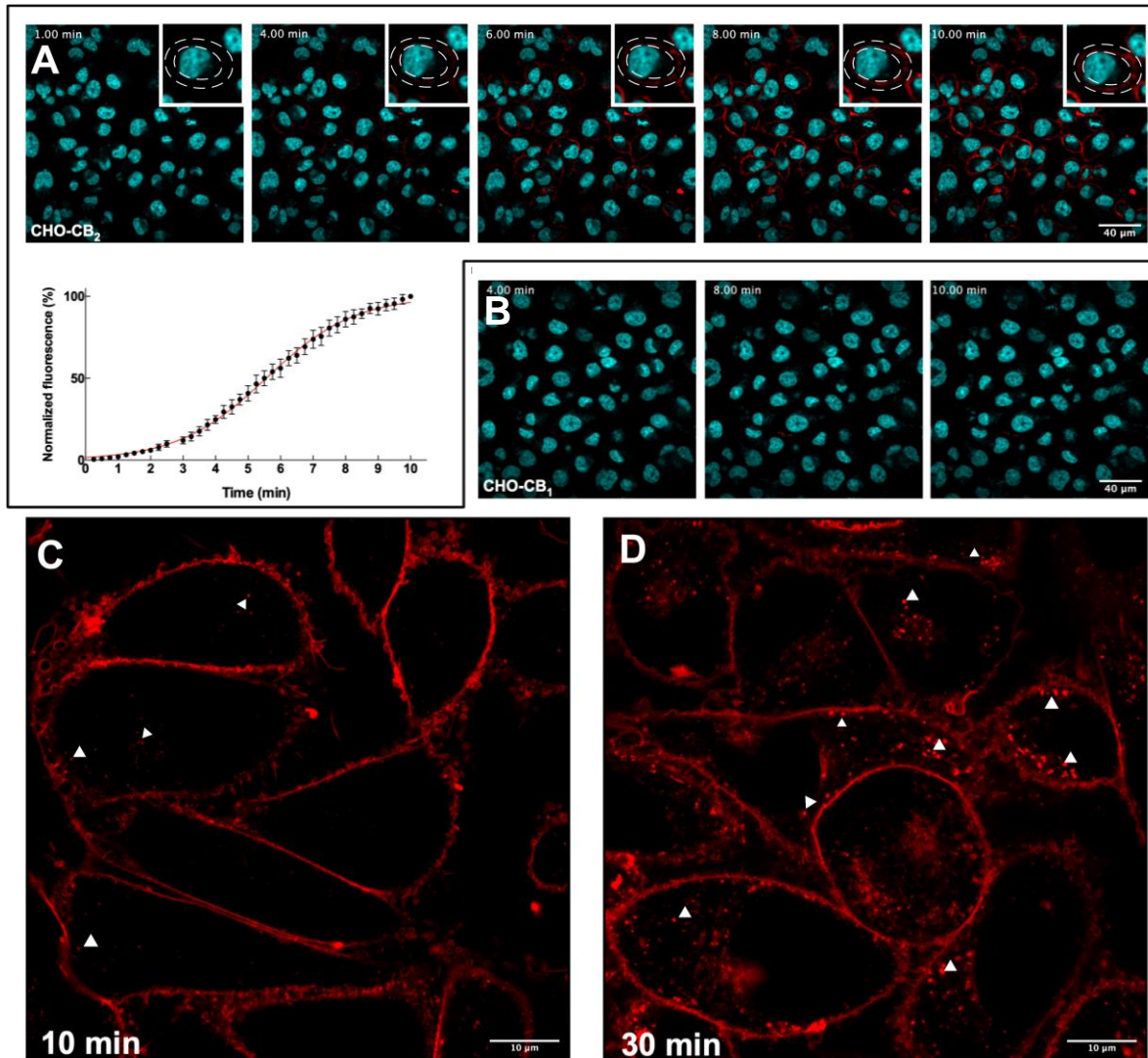
1)

Figure 6. Confocal Fluorescence Microscopy with CHO cells. Different frames from time-lapse confocal microscopy of cells co-stained with **3b** (red) and Hoechst 33342 (cyan, nucleus counter stain). A) CHO-hCB$_2$R cells incubated with 0.2 µM **3b** at 1, 4, 6, 8 and 10 min.; at each time point, a region of interest (white strip-like curve shown in the inserts) was drawn around the plasma membrane of cells (N = 6 for each field). The changes in normalized fluorescence intensity were estimated over time (Fiji software), leading to an association curve. The data on the

curve represent the mean ± S.D. of at least three independent experiments. B) CHO-hCB$_1$R cells incubated with 0.2 μM **3b** at 4, 8 and 10 min. See supplementary movie 1 and 2 for animated views. Airyscan high-resolution imaging of hCB$_2$R-overexpressing CHO cells incubated for either C) 10 min or D) 30 min with 0.2 μM **3b**. Cells were optically sectioned using confocal laser-scanning microscopy equipped with an Airyscan detector. C) In the first 10 min, **3b** staining was localized in the plasma membranes of CHO-hCB$_2$R cells. D) After 30 min, brighter and increased number of vesicles, reminiscent of early endosomes appeared below the plasma membrane and within the cytosol. Images are representative of three independent experiments.
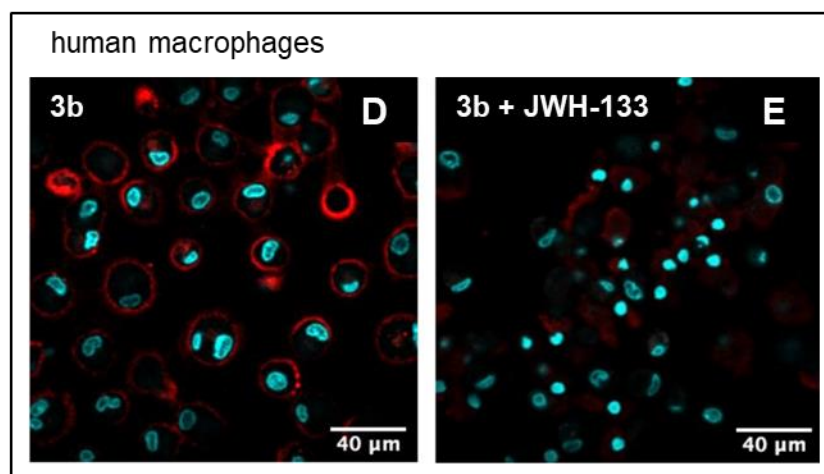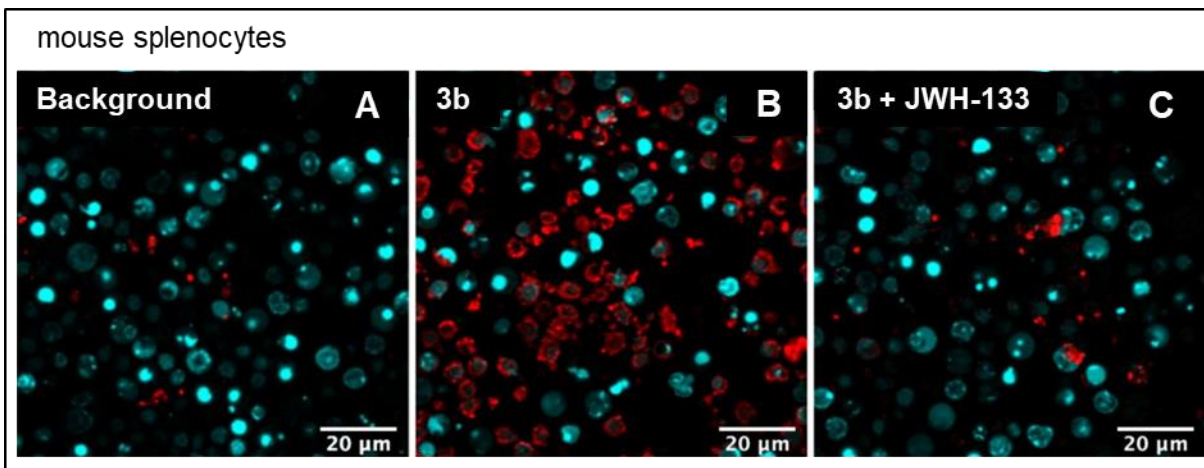
Figure 7. Confocal microscopy with primary cells expressing CB₂R endogenously. Confocal microscopy frames that show labeling of CB₂R with **3b** in murine splenocytes and human macrophages. Murine splenocytes incubated for 10 min with A) vehicle, B) 0.4 μM **3b** alone or C) in presence of 4 μM known CB₂R agonist JWH-133 as competitor. Human macrophages stained for 10 min with D) 0.6 μM **3b** alone or E) in presence of 4 μM JWH-133. Pre-treatment with Hoechst 33342 (cyan) effected nuclear counter-staining.

Of note, **3b** was only weakly fluorescent in aqueous media, allowing bright labeling of cell membrane even in the continued presence of the probe in culture medium. As a control, at concentrations up to 0.6 μM **3b** did not produce membrane labeling of CHO cells overexpressing hCB₁R, demonstrating the high specificity of this ligand for hCB₂R as well as its particularly low nonspecific binding (Fig. 6B, also see Supplementary Video 2). Image acquisition at higher magnification and resolution was performed at the end of the recording session. After 10 min of probe administration, cell staining remained predominantly associated with the plasma membrane (Fig. 6C). However, after 30 min a high number of small spots was observed on the cytoplasmic side of the cell membrane as well as throughout the cytoplasm, suggesting agonist-mediated endocytosis (Fig. 6D). Consistently, **3b**-induced internalization of hCB₂R was almost completely blocked in presence of endocytosis inhibitors (see SI Fig. S8). Incidentally, these findings confirmed that **3b**, which exhibited a P_{eff} of 0.4 cm/s·10^{-6} in PAMPA assay,[68] is poorly membrane-permeant. Consequently, **3b** is suitable for labeling hCB₂R on membranes for longer periods with minimal interference of agonist-mediated internalization.

Having established its suitability in cells overexpressing hCB₂R, we also investigated the potential of **3b** for primary, non-transfected cells expressing the receptor at native levels. In this context, **3b** brightly labeled mouse splenocytes (Fig. 7B) and human macrophages (Fig. 7E) in a time-dependent manner. In the presence of CB₂R-specific agonist JWH-133, drastic reduction of fluorescent labeling confirmed CB₂R-specificity (Fig. 7C and 7E) and Supporting Videos 3 - 7). To the best of our knowledge, such specificity in living cells expressing CB₂R endogenously is unprecedented for CB₂R fluorescent probes, underscoring the (pre)-clinical promise of this probe. Collectively, these data demonstrate that DY-480XL probe **3b** is ideally suited for membrane-bound CB₂R real-time imaging with exceedingly low levels of nonspecific binding.

Conclusion

In conclusion, a series of CB$_2$R selective fluorescent probes was synthesized, characterized and cross-validated in multiple laboratories, in order to maximize the chance for successful translation of preclinical applications. Our collaborative efforts led to the identification of reliable tools for flow cytometry and time-resolved confocal microscopy with living human and murine cells expressing CB$_2$R. Moreover, evaluation of equilibrium and kinetic binding parameters were performed in a novel TR-FRET-based assay, which is amenable to high throughput screening. Probes bearing DY-480XL (**3b**), Alexa488 (**5**) and AttoThio12 (**6**) dyes emerged as the most promising in terms of *in vitro* pharmacology, showing nanomolar affinity to hCB$_2$R and good to excellent selectivity over hCB$_1$R. Probes **3b** and **6** were used for determination of K$_i$ values and evaluation of ligand binding kinetics of competing ligands by TR-FRET, and thus they can be used as alternatives to radioligands. Probes **3b**, **4**, and **5** specifically labeled mouse and human CB$_2$R-positive cell populations over a broad concentration range in FACS analysis. Target specificity was established by the first report of successful competition experiments with well-known CB$_2$R ligands (agonist and inverse agonist). Importantly, **3b** could be applied to the detection of endogenous CB$_2$R levels such as mCB$_2$R on activated AD mouse microglia as well as hCB$_2$R in human breast MDA-MB-231 cancer cells. Lastly, **3b** was successfully utilized to label and monitor live cells overexpressing hCB$_2$R by real-time confocal fluorescence microscopy over prolonged time with minimal internalization. In particular, **3b** specifically labeled mCB$_2$R on mouse splenocytes and hCB$_2$R on macrophages, highlighting the translational promise of these probes, as well as their potential for direct receptor detection, a long sought-after goal for which so far no reliable tools have been available. Consequently, **3b** is a privileged fluorescent probe for visualizing both human and murine living cells expressing CB$_2$R endogeneously, and it may help answer fundamental questions concerning CB$_2$R expression in health and disease.

Considering the wealth of questions regarding CB$_2$R expression and function in so many different cells and tissues, it is likely that a single fluorescent probe will not meet the requirements of any given experiment. In that regard, amine platform **1** was shown to be privileged for the preparation of a collection of fluorescent ligands specifically targeting CB$_2$R. Hence, **1** should serve as linchpin for additional probes with bespoke pharmacological and photophysical properties. We believe the probes described herein are valuable research tools for practitioners in the field. They should find widespread use to foster better understanding of CB$_2$R in health and disease and to ultimately unlock the receptor's therapeutic potential.

AUTHOR INFORMATION

Corresponding Author

*E-mail: erickm.carreira@org.chem.ethz.ch

*E-mail: uwe.grether@roche.com

Notes
The authors declare no competing financial interest.

REFERENCES

(1)   Marzo, V. D.; Bifulco, M.; Petrocellis, L. D. *Nat. Rev. Drug Discov.* **2004**, *3* , 771.

(2)   Matsuda, L. A.; Lolait, S. J.; Brownstein, M. J.; Young, A. C.; Bonner, T. I. *Nature* **1990**, *346*, 561.

(3)   Munro, S.; Thomas, K. L.; Abu-Shaar, M. *Nature* **1993**, *365*, 61.

(4)   Maccarrone, M.; Bab, I.; Bíró, T.; Cabral, G. A.; Dey, S. K.; Di Marzo, V.; Konje, J. C.; Kunos, G.; Mechoulam, R.; Pacher, P.; Sharkey, K. A.; Zimmer, A. *Trends Pharmacol. Sci.* **2015**, *36* , 277.

(5)   Izzo, A. A.; Borrelli, F.; Capasso, R.; Marzo, V. D.; Mechoulam, R. *Trends Pharmacol. Sci.* **2009**, *30*, 515.

(6)   Galiègue, S.; Mary, S.; Marchand, J.; Dussossoy, D.; Carrière, D.; Carayon, P.; Bouaboula, M.; Shire, D.; LE Fur, G.; Casellas, P. *Eur. J. Biochem.* **1995**, *232*, 54.

(7)   Turcotte, C.; Blanchet, M.-R.; Laviolette, M.; Flamand, N. *Cell. Mol. Life Sci.* **2016**, *73*, 4449.

(8)   Pacher, P.; Mechoulam, R. *Prg Lipid Res.* **2011**, *50*, 193.

(9)   Guindon, J.; Hohmann, A. G. C *Br. J. Pharmacol.* **2008**, *153*, 319.

(10)   Pacher, P.; Kunos, G. M. *FEBS J.* **2013**, *280*, 1918.

(11)   Dhopeshwarkar, A.; Mackie, K. *Mol. Pharmacol.* **2014**, *86*, 430.

(12)   Han, S.; Thatte, J.; Buzard, D. J.; Jones, R. M. *J. Med. Chem.* **2013**, *56*, 8224.

(13)   Marchalant, Y.; Brownjohn, P. W.; Bonnet, A.; Kleffmann, T.; Ashton, J. C. *J. Histochem. Cytochem.* **2014**, *62*, 395.

(14)   Zhang, H.-Y.; Shen, H.; Jordan, C. J.; Liu, Q.-R.; Gardner, E. L.; Bonci, A.; Xi, Z.-X. *Acta Pharmacol. Sin.* **2019**, *40*, 398.

(15)   Cécyre, B.; Thomas, S.; Ptito, M.; Casanova, C.; Bouchard, J.-F. *Naunyn-Schmiedeberg's Arch. Pharmacol.* **2014**, *387*, 175.

(16)   Cabral, G. A.; Marciano-Cabral, F. *J. Leukoc. Biol.* **2005**, *78*, 1192.

(17)   Ashton, J. C.; Glass, M. T. *Curr. Neuropharmacol.* **2007**, *5*, 73..

(18)   Grimsey, N. L.; Goodfellow, C. E.; Dragunow, M.; Glass, M. *Biochim. Biophys. Acta (BBA) - Molecular Cell Research* **2011**, *1813*, 1554.

(19)   Soethoudt, M.; Grether, U.; Fingerle, J.; Grim, T. W.; Fezza, F.; Petrocellis, L. de; Ullmer, C.; Rothenhäusler, B.; Perret, C. *et al. Nat. Commun.* **2017**, *8*, 13958.

(20)   Stoddart, L. A.; Kilpatrick, L. E.; Briddon, S. J.; Hill, S. J. *Neuropharmacology* **2015**, *98*, 48.

(21)   Vernall, A. J.; Hill, S. J.; Kellam, B. *Br. J. Pharmacol.* **2014**, *171*, 1073.

(22)   Iliopoulos-Tsoutsouvas, C.; Kulkarni, R. N.; Makriyannis, A.; Nikas, S. P. *Expert Opin Drug Discov.* **2018**, *13*, 933.

(23)   Bai, M.; Sexton, M.; Stella, N.; Bornhop, D. J. *Bioconjug. Chem.* **2008**, *19*, 988.

(24)   Sexton, M.; Woodruff, G.; Horne, E. A.; Lin, Y. H.; Muccioli, G. G.; Bai, M.; Stern, E.; Bornhop, D. J.; Stella, N. *Cell Chem. Biol.* **2011**, *18*, 563.

(25)   Petrov, R. R.; Ferrini, M. E.; Jaffar, Z.; Thompson, C. M.; Roberts, K.; Diaz, P. *B Bioorg. Med. Chem. Lett.* **2011**, *21*, 5859.

(26)   Martín-Couce, L.; Martín-Fontecha, M.; Capolicchio, S.; López-Rodríguez, M. L.; Ortega-Gutiérrez, S. *J. Med. Chem.* **2011**, *54*, 5265.

(27)   Zhang, S.; Shao, P.; Bai, M. *Bioconjug. Chem.* **2013**, *24*, 1907.

(28)   Wu, Z.; Shao, P.; Zhang, S.; Bai, M. *J. Biomed. Opt.* **2014**, *19*, 36006.

(29)   Zhang, S.; Jia, N.; Shao, P.; Tong, Q.; Xie, X.-Q.; Bai, M. *Chem. Biol.* **2014**, *21*, 338.

(30)   Ling, X.; Zhang, S.; Shao, P.; Li, W.; Yang, L.; Ding, Y.; Xu, C.; Stella, N.; Bai, M. A. *Biomaterials* **2015**, *57*, 169.

(31)   Zubiaurre, A. R. **2016** Chemical Probes for the Study of the Endogenous Cannabinoid System (Doctoral dissertation) Universidad Complutense de Madrid, Spain.

(32)   Cooper, A. G.; Oyagawa, C. R. M.; Manning, J. J.; Singh, S.; Hook, S.; Grimsey, N. L.; Glass, M.; Tyndall, J. D. A.; Vernall, A. J. *Med. Chem. Commun.* **2018**, *9*, 2055.

(33)   Cooper, A. G.; MacDonald, C.; Glass, M.; Hook, S.; Tyndall, J. D. A.; Vernall, A. J. *Eur. J. Med. Chem.* **2018**, *145*, 770.

(34)   Spinelli, F.; Giampietro, R.; Stefanachi, A.; Riganti, C.; Kopecka, J.; Abatematteo, F. S.; Leonetti, F.; Cola-bufo, N. A.; Mangiatordi, G. F.; Nicolotti, O.; Perrone, M. G.; Brea, J.; Loza, M. I.; Infantino, V.; Abate, C.; Contino, M. *Eur. J. Med. Chem.* **2020**, *188*, 112037.

(35)   Singh, S.; Oyagawa, C. R. M.; Macdonald, C.; Grimsey, N. L.; Glass, M.; Vernall, A. J. *ACS Med. Chem. Lett.* **2019**, *10*, 209.

(36)   Martín-Couce, L.; Martín-Fontecha, M.; Palomares, Ó.; Mestre, L.; Cordomí, A.; Hernangomez, M.; Palma, S.; Pardo, L.; Guaza, C.; López-Rodríguez, M. L.; Ortega-Gutiérrez, S. *Angew. Chem. Int. Ed.* **2012**, *51*, 6896.

(37)   Soethoudt, M.; Stolze, S. C.; Westphal, M. V.; van Stralen, L.; Martella, A.; van Rooden, E. J.; Guba, W.; Varga, Z. V.; Deng, H.; van Kasteren, S. I.; Grether, U.; IJzerman, A. P.; Pacher, P.; Carreira, E. M.; Overkleeft, H. S.; Ioan-Facsinay, A.; Heitman, L. H.; van der Stelt, M. *J. Am. Chem. Soc.* **2018**, *140*, 6067.

(38)   Hanuš, L.; Breuer, A.; Tchilibon, S.; Shiloah, S.; Goldenberg, D.; Horowitz, M.; Pertwee, R. G.; Ross, R. A.; Mechoulam, R.; Fride, E. *Proc. Natl. Acad. Sci. U S A* **1999**, *96*, 14228.

(39)   Westphal, M. V.; Sarott, R. C.; Zirwes, E. A.; Osterwald, A.; Guba, W.; Ullmer, C.; Grether, U.; Carreira, E. M. Highly Selective, Amine-Derived Cannabinoid Receptor 2 Probes. *Chem. Eur. J.* **2020**, *26*, 1380.

(40)   Ma, Z.; Du, L.; Li, M. *J. Med. Chem.* **2014**, *57*, 8187.

(41)   Leopoldo, M.; Lacivita, E.; Berardi, F.; Perrone, R. *Drug Discov. Today* **2009**, *14*, 706.

(42)   Mazères, S.; Schram, V.; Tocanne, J. F.; Lopez, A. *Biophys. J.* **1996**, *71*, 327.

(43) Comerci, C. J.; Herrmann, J.; Yoon, J.; Jabbarpour, F.; Zhou, X.; Nomellini, J. F.; Smit, J.; Shapiro, L.; Wakatsuki, S.; Moerner, W. E. *Nat. Commun.* **2019**, *10*, 1–10.

(44) Berlier, J. E.; Rothe, A.; Buller, G.; Bradford, J.; Gray, D. R.; Filanoski, B. J.; Telford, W. G.; Yue, S.; Liu, J.; Cheung, C.-Y.; Chang, W.; Hirsch, J. D.; Beechem Rosaria P. Haugland, J. M.; Haugland, R. P. *J. Histochem. Cytochem.* **2003**, *51*, 1699.

(45) Lindhoud, S.; Westphal, A. H.; Visser, A. J. W. G.; Borst, J. W.; Mierlo, C. P. M. van. *PLOS ONE* **2012**, *7*, e46838.

(46) Chmyrov, A.; Arden-Jacob, J.; Zilles, A.; Drexhage, K.-H.; Widengren, J. *Photochem. Photobiol. Sci.* **2008**, *7*, 1378.

(47) PDB 5ZTY: Li, X.; Hua, T.; Vemuri, K.; Ho, J.-H.; Wu, Y.; Wu, L.; Popov, P.; Benchama, O.; Zvonok, N.; Locke, K.; Qu, L.; Han, G. W.; Iyer, M. R.; Cinar, R.; Coffey, N. J.; Wang, J.; Wu, M.; Katritch, V.; Zhao, S.; Kunos, G.; Bohn, L. M.; Makriyannis, A.; Stevens, R. C.; Liu, Z.-J. *Cell* **2019**, *176*, 459.

(48) PDB 6PT0: Xing, C.; Zhuang, Y.; Xu, T.-H.; Feng, Z.; Zhou, X. E.; Chen, M.; Wang, L.; Meng, X.; Xue, Y.; Wang, J.; Liu, H.; McGuire, T. F.; Zhao, G.; Melcher, K.; Zhang, C.; Xu, H. E.; Xie, X.-Q. *Cell* **2020**, *180,* 645.

(49) Unfortunately, our consortium does not have a mCB$_1$R binding assay in place. Consequently, we were not able to generate murine receptor selectivity (mCB$_2$R vs mCB$_1$R) data. However, the amino acid sequences of hCB$_1$R and mCB$_1$R binding pockets only differ in one residue, Ile105 (h) as opposed to Met (m). For probes showing good selectivity for hCB$_2$R, similar selectivity can be expected also for murine receptors. Liu, Q.-R.; Pan, C.-H.; Hishimoto, A.; Li, C.-Y.; Xi, Z.-X.; Llorente-Berzal, A.; Viveros, M.-P.; Ishiguro, H.; Arinami, T.; Onaivi, E. S.; Uhl, G. R. *Genes Brain Behav.* **2009**, *8*, 519.

(50) Bendels, S.; Bissantz, C.; Fasching, B.; Gerebtzoff, G.; Guba, W.; Kansy, M.; Migeon, J.; Mohr, S.; Peters, J.-U.; Tillier, F.; Wyler, R.; Lerner, C.; Kramer, C.; Richter, H.; Roberts, S. *J. Pharmacol. Tox. Met.* **2019**, 106609.

(51) Martella, A.; Sijben, H.; Rufer, A. C.; Grether, U.; Fingerle, J.; Ullmer, C.; Hartung, T.; IJzerman, A. P.; Stelt, M. van der; Heitman, L. H. *Mol. Pharmacol.* **2017**, *92*, 389.

(52) Albizu, L.; Teppaz, G.; Seyer, R.; Bazin, H.; Ansanay, H.; Manning, M.; Mouillac, B.; Durroux, T. *J. Med. Chem.* **2007**, *50*, 4976.

(53) Loison, S.; Cottet, M.; Orcel, H.; Adihou, H.; Rahmeh, R.; Lamarque, L.; Trinquet, E.; Kellenberger, E.; Hibert, M.; Durroux, T.; Mouillac, B.; Bonnet, D. *J. Med. Chem.* **2012**, *55*, 8588.

(54) Zwier, J. M.; Roux, T.; Cottet, M.; Durroux, T.; Douzon, S.; Bdioui, S.; Gregor, N.; Bourrier, E.; Oueslati, N.; Nicolas, L.; Tinel, N.; Boisseau, C.; Yverneau, P.; Charrier-Savournin, F.; Fink, M.; Trinquet, E. *J. Biomol. Screen* **2010**, *15*, 1248.

(55) Leyris, J.-P.; Roux, T.; Trinquet, E.; Verdié, P.; Fehrentz, J.-A.; Oueslati, N.; Douzon, S.; Bourrier, E.; Lamarque, L.; Gagne, D.; Galleyrand, J.-C.; M'kadmi, C.; Martinez, J.; Mary, S.; Banères, J.-L.; Marie, J. *Anal. Biochem.* **2011**, *408*, 253.

(56) Martinez-Pinilla, E.; Rabal, O.; Reyes-Resina, I.; Zamarbide, M.; Navarro, G.; Sanchez-Arias, J. A.; de Miguel, I.; Lanciego, J. L.; Oyarzabal, J.; Franco, R. *J. Pharmacol. Exp. Ther.* **2016**, *358*, 580.

(57) Copeland, R. A.; Pompliano, D. L.; Meek, T. D. *Nat. Rev. Drug Discov.* **2006**, *5*, 730.

(58) Swinney, D. C. *Curr. Opin. Drug Discov. Devel.* **2009**, *12* , 31.

(59) Lu, H.; Tonge, P. J. Drug-Target Residence Time: C*Curr. Opin. Chem. Biol.* **2010**, *14*, 467.

(60) Lane, J. R.; May, L. T.; Parton, R. G.; Sexton, P. M.; Christopoulos, A. *Nat. Chem. Biol.* **2017**, *13*, 929.

(61) Klein Herenbrink, C.; Sykes, D. A.; Donthamsetti, P.; Canals, M.; Coudrat, T.; Shonberg, J.; Scammells, P. J.; Capuano, B.; Sexton, P. M.; Charlton, S. J.; Javitch, J. A.; Christopoulos, A.; Lane, J. R. *Nat. Commun.* **2016**, *7*, 10842.

(62) van der Velden, W. J. C.; Heitman, L. H.; Rosenkilde, M. M. Perspective: Implications of Ligand–Receptor Binding Kinetics for Therapeutic Targeting of G Protein-Coupled Receptors. *ACS Pharmacol. Transl. Sci.* **2020**, *3*, 179.

(63) Rinaldi-Carmona, M.; Barth, F.; Millan, J.; Derocq, J.-M.; Casellas, P.; Congy, C.; Oustric, D.; Sarran, M.; Bouaboula, M.; Calandra, B.; Portier, M.; Shire, D.; Brelière, J.-C.; Fur, G. L. *J. Pharmacol. Exp. Ther.* **1998**, *284*, 644.

(64) Bosch, P. J.; Corrêa, I. R.; Sonntag, M. H.; Ibach, J.; Brunsveld, L.; Kanger, J. S.; Subramaniam, V. E *Biophys. J.* **2014**, *107*, 803.

(65) Ouali Alami, N.; Schurr, C.; Olde Heuvel, F.; Tang, L.; Li, Q.; Tasdogan, A.; Kimbara, A.; Nettekoven, M.; Ottaviani, G.; Raposo, C.; Röver, S.; Rogers-Evans, M.; Rothenhäusler, B.; Ullmer, C.; Fingerle, J.; Grether, U.; Knuesel, I.; Boeckers, T. M.; Ludolph, A.; Wirth, T.; Roselli, F.; Baumann, B. *The EMBO J.* **2018**, *37*, e98697.

(66)   Oakley, H.; Cole, S. L.; Logan, S.; Maus, E.; Shao, P.; Craft, J.; Guillozet-Bongaarts, A.; Ohno, M.; Dister-hoft, J.; Eldik, L. V.; Berry, R.; Vassar, R. *J. Neurosci.* **2006**, *26*, 10129.

(67)   López, A.; Aparicio, N.; Pazos, M. R.; Grande, M. T.; Barreda-Manso, M. A.; Benito-Cuesta, I.; Vázquez, C.; Amores, M.; Ruiz-Pérez, G.; García-García, E.; Beatka, M.; Tolón, R. M.; Dittel, B. N.; Hillard, C. J.; Romero, J. *J. Neuroinflammation* **2018**, *15*, 158.

(68)   Kansy, M.; Senner, F.; Gubernator, K. Physicochemical *J. Med. Chem.* **1998**, *41*, 1007.